7 - 12 SEPTEMBER 2014, KRAKÓW
FORUM ACUSTICUM

Wave propagation and attenuation in wool felt

Dmitri Kartofelev, Anatoli Stulov
Laboratory of Nonlinear Dynamics, Institute of Cybernetics at Tallinn University of Technology, Tallinn, Estonia.

Summary
Based on the experimental data of the piano hammers study, the one-dimensional nonlinear constitutive equation of the felt material is derived. A nonlinear partial differential equation with third order terms that takes into account the elastic and hereditary properties of a microstructured wool felt is used to study the evolution of initial disturbance in the felt material. The physical dimensionless parameters are established and their importance in describing the nonlinear effects is discussed. The initial and boundary value problems are considered, and the numerical solution describing the nonlinear wave propagation is provided. The influence of the felt nonlinearity is examined. It is demonstrated that the nonlinearity makes the front slope of a pulse steeper, which causes the eventual breaking of the propagating wave. Also, we provided a detailed dispersion analysis of the linear problem, and estimate the rate of the wave attenuation in the felt material. In addition, it is shown that for special values of physical parameters the wave components with a negative group velocity appear.

PACS no. 43.25.Zx, 43.40.Cw, 43.75.Gh, 43.40.At

1. Introduction

The aim of this paper is to explore one of the oldest microstructured material known to man. This remarkable material is the felt. The felt is produced of randomized fibres that are tightly matted together. It can be made of natural fibres such as wool or synthetic fibres such as acrylic. The felt is used almost everywhere from the automotive industry, to the construction of musical instruments. Some applications of the felt include vibration isolation, air filtering, and interior décor. For almost two centuries, the felt has been used in piano manufacturing. For instance, the piano string dampers are made using felt and, of course, the felt made of wool is a unique and indispensable coating matter of piano hammers.

In this paper a brief description of the model of wool felt proposed in [1] is presented. The model involves a one-dimensional nonlinear constitutive equation of microstructured felt based on the experimental results of the piano hammers testing.

Below, we investigate the evolution of the form of a pulse propagating trough a one-dimensional nonlinear felt media. A detailed dispersion analysis, of the linear problem is provided. It is shown that for special values of physical parameters the spectral wave components with a negative group velocity appear. The rate of attenuation of a propagating pulse is estimated and discussed.

2. Wool felt model

The first nonlinear dynamical model of the piano hammer felt, which takes into consideration both the hysteresis of the force-compression characteristics, and their dependence on the rate of the felt loading was presented in [2]. The derived model is based on the assumption that the hammer felt is a microstructured material possessing history-dependent properties, i.e. it is a material with memory.

The constitutive equation of nonlinear microstructured wool felt may be assumed in the form

$$\sigma(\epsilon) = E\epsilon^p(t). \tag{1}$$

Here σ is the stress, $\epsilon = \partial u/\partial x$ is the strain, u is the displacement, E is Young's modulus, and p is the nonlinearity parameter.

Following Rabotnov [3], the constitutive equation of microstructured wool felt is derived by replacing the constant value of Young's modulus E in expression (1) by a time-dependent operator $E_d\,[1 - \mathcal{R}(t)*]$, where $*$ denotes the convolution operation, and the relaxation function is given by

$$\mathcal{R}(t) = \frac{\gamma}{\tau_0}\, e^{-t/\tau_0}, \quad 0 \leqslant \gamma < 1. \tag{2}$$

Here the hereditary amplitude γ and relaxation time τ_0 are the hereditary parameters of the wool felt. The time history of the felt deformation is assumed to start at $t = 0$. This means that for the case of one-dimensional deformation and for any rate of loading the hysteretic felt material is defined by the constitutive equation

$$\sigma(\epsilon) = E_d \left[\epsilon^p(t) - \mathcal{R}(t) * \epsilon^p(t)\right], \tag{3}$$

where constant E_d is the dynamic Young's modulus. From Eq. (3) it follows that if $t \ll \tau_0$ then one obtains the constitutive equation for the fast felt compression

$$\sigma(\epsilon) = E_d \epsilon^p(t), \tag{4}$$

and if $t \gg \tau_0$ then we have the constitutive equation for the slow compression

$$\sigma(\epsilon) = E_d(1-\gamma)\epsilon^p(t) = E_s \epsilon^p(t). \tag{5}$$

In each of these two cases, the loading and unloading of the felt follows the same path. The quantity $E_s = E_d(1-\gamma)$ is the static Young's modulus of the felt material. Both Young's moduli are physical parameters of the felt material, and their values are $0 < E_s < \infty$, and $0 < E_d < \infty$. For this reason, within the frame of the felt model, the value of the hereditary amplitude is always $\gamma < 1$.

The governing equation, which describes the evolution of the one-dimensional wave in the felt material is derived from the classical equation of motion

$$\rho \frac{\partial^2 u}{\partial t^2} = \frac{\partial \sigma}{\partial x}, \tag{6}$$

where ρ is the density of the medium. Substitution of (3) in Eq. (6) and elimination of the integral term leads to the equation in the following form, presented in terms of the displacement u

$$\rho u_{tt} + \rho\tau_0 u_{ttt} - E_d \left\{(1-\gamma)\left[(u_x)^p\right]_x + \tau_0 \left[(u_x)^p\right]_{xt}\right\} = 0, \tag{7}$$

where the subscripted indices denote the differentiation with respect to indicated variables.

One can derive the dimensionless form of Eq. (7) by using the dimensionless variables

$$u \Rightarrow \frac{u}{l_0}, \quad x \Rightarrow \frac{x}{l_0}, \quad t \Rightarrow \frac{t}{\alpha_0}, \tag{8}$$

where

$$\alpha_0 = \frac{\tau_0}{\delta}, \quad l_0 = c_d \alpha_0 \sqrt{\delta}, \quad \delta = 1-\gamma, \quad c_d = \sqrt{\frac{E_d}{\rho}}, \quad c_s = c_d\sqrt{\delta}. \tag{9}$$

Thus, Eq. (7) in terms of dimensionless displacement variable $u(x,t)$ takes the following form:

$$\left[(u_x)^p\right]_x - u_{tt} + \left[(u_x)^p\right]_{xt} - \delta u_{ttt} = 0, \tag{10}$$

and for the strain variable $\epsilon(x,t)$ Eq. (7) reads

$$(\epsilon^p)_{xx} - \epsilon_{tt} + (\epsilon^p)_{xxt} - \delta\epsilon_{ttt} = 0. \tag{11}$$

Several samples of felt pads were subjected to static stress-strain tests. The average value of the static Young's modulus of the felt pads was estimated to be $E_s = 0.6$ MPa. The average value of the felt density was determined as $\rho \approx 10^3$ kg/m^3. By using the realistic values of hereditary parameters $\gamma = 0.96$ and $\tau_0 = 10$ μs presented in [4], we obtain

$$\delta = 0.04, \quad E_d = 15 \text{ MPa}, \quad c_s = 25 \text{ m/s}, \quad c_d = 125 \text{ m/s}. \tag{12}$$

For these values of material constants, the space scale l_0 and time scale α_0 used in (8) follow

$$l_0 = 6.25 \text{ mm}, \quad \alpha_0 = 0.25 \text{ ms}. \tag{13}$$

3. Linear analysis

3.1. Dispersion relation

The peculiar characteristics of the solution of Eq. (11) are already revealed in the linear case, where $p = 1$

$$\epsilon_{xx} - \epsilon_{tt} + \epsilon_{xxt} - \delta\epsilon_{ttt} = 0. \tag{14}$$

The fundamental solution of this equation has the form of traveling waves

$$\epsilon(x,t) = \hat{\epsilon} e^{ikx - i\Omega t}, \tag{15}$$

where i is an imaginary unit, k is the wave number, Ω is the angular frequency, and $\hat{\epsilon}$ is the amplitude. The dispersion law $\Phi(k,\Omega) = 0$ of Eq. (14) is defined by relation

$$k^2 - \Omega^2 - ik^2\Omega + i\delta\Omega^3 = 0. \tag{16}$$

In the case of an initial value problem, the general solution of Eq. (14) has the following form:

$$\epsilon(x,t) = \frac{1}{2\pi}\int_{-\infty}^{\infty} \chi(k) e^{ikx - i\Omega(k)t} dk, \tag{17}$$

where $\chi(k)$ is the Fourier transform of the initial disturbance of the strain prescribed at $t = 0$. The dependence $\Omega = \Omega(k)$ can be derived from the dispersion relation (16). In the general case $\Omega(k)$ is a complex quantity. In order to provide the dispersion analysis in the context of an initial value problem, and in the complex number domain, we rewrite the frequency $\Omega(k)$ in the form

$$\Omega(k) = \omega(k) + i\mu(k), \tag{18}$$

where $\omega = \mathrm{Re}(\Omega)$ and $\mu = \mathrm{Im}(\Omega)$. By using this notation, expression (15) can be rewritten as follows:

$$\epsilon(x,t) = \hat{\epsilon}\, e^{ikx - i\omega t + \mu t} = e^{\mu t}\, \hat{\epsilon} e^{ikx - i\omega t}. \tag{19}$$

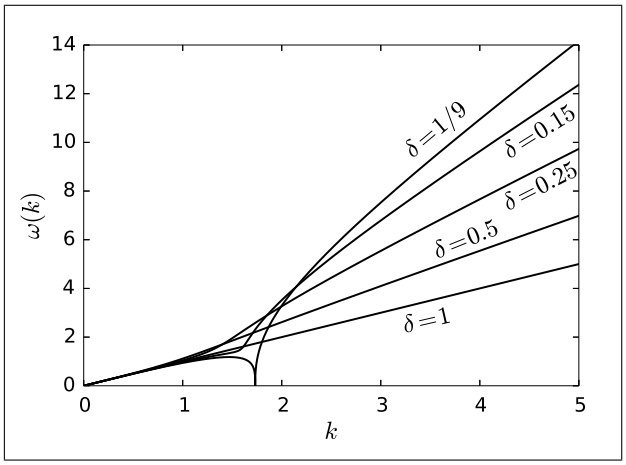

Figure 1. Dispersion curves $\omega(k)$ calculated for different values of material parameter δ.

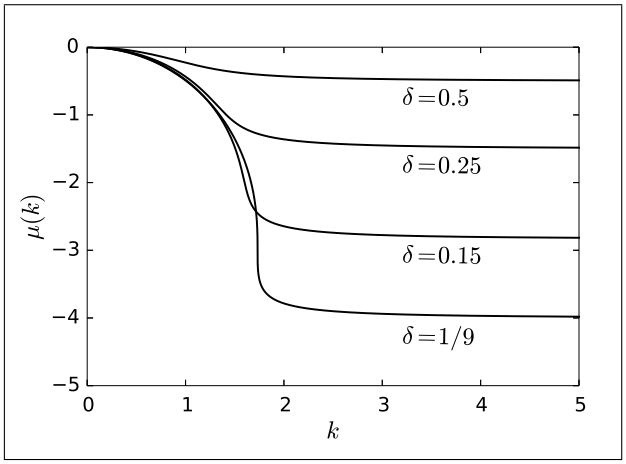

Figure 2. Dispersion curves $\mu(k)$ calculated for different values of material parameter δ.

From here it is evident that for the negative values of $\mu(k)$ it acts as an exponential decay function. In other words, the spectral components decay exponentially as $t \to \infty$ for $\mu(k) < 0$. On the other hand, if $\mu(k) > 0$, then the amplitude of the corresponding spectral component increases exponentially with the progression of time, and the solution of the Eq. (14) becomes unstable.

By taking into account (18), the dispersion relation (16) takes the following form:

$$k^2 - ik^2\omega - \omega^2 + i\delta\omega^3 + k^2\mu - 2i\omega\mu - 3\delta\omega^2\mu + \mu^2 - 3i\delta\omega\mu^2 + \delta\mu^3 = 0. \quad (20)$$

The dispersion relation (20) can be separated into real and imaginary parts. the solution of that simultaneous equation with respect to ω and μ has the following form:

$$\begin{cases} \omega = \dfrac{\sqrt{6}}{12\delta S}\sqrt{\sqrt[3]{2}S^4 - 4S^2(1-3k^2\delta) + 2\sqrt[3]{4}(1-3k^2\delta)^2}, \\ \mu = \dfrac{1}{12\delta S}\left[\sqrt[3]{4}S^2 - 4S + 2\sqrt[3]{2}(1-3k^2\delta)\right], \end{cases} \quad (21)$$

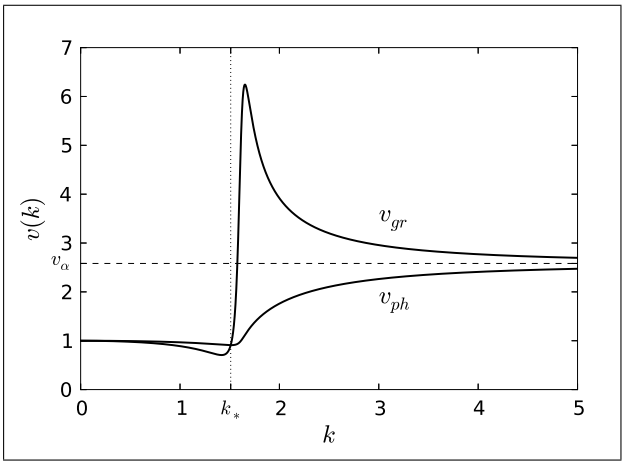

Figure 3. Phase and group velocities calculated for $\delta = 0.15$. Vertical dotted line at k_* separates the regions of normal and anomalous dispersion.

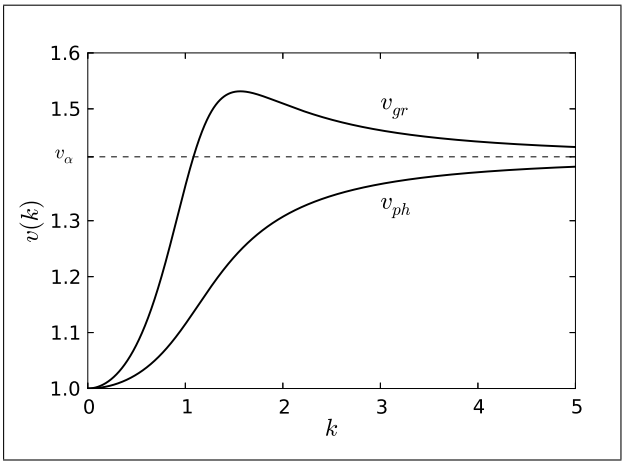

Figure 4. Phase and group velocities calculated for $\delta = 0.5$.

where

$$S = \sqrt[3]{2 - 9k^2\delta(1-3\delta) + 3k\delta\sqrt{3Q}}, \quad (22)$$

$$Q = 4k^4\delta - k^2(1 + 18\delta - 27\delta^2) + 4. \quad (23)$$

This solution is physically reasonable, because it satisfies the conditions $\omega \in \mathbb{R}$, $\mu \in \mathbb{R}$, and $\mu \leqslant 0$. It can be shown that the solution (21) has three distinct modes of behaviour, which depend on the value of the parameter δ. These three solution regimes correspond to the following values of δ: (i) $0 < \delta \leqslant 1/9$; (ii) $1/9 < \delta < 1$; and (iii) $\delta = 1$.

Figures 1 and 2 show the examples of the dispersion curves for the case (ii). The dispersion curves are continuous functions, and one can notice that as the parameter δ becomes larger the dispersion curve $\omega(k)$ becomes more similar to the dispersion curve of the non-dispersive medium ($\omega(k) = k$, $\mu(k) = 0$). Also, the average value of the exponential decay function $\mu(k)$ becomes progressively smaller, with the increasing of the value of parameter δ, especially for the

larger k values. Figure 2 shows that the decay function $\mu(k)$ is more or less constant if $k > 2$. The limits of dispersion relations $\omega(k)$ and $\mu(k)$ for large k are

$$\lim_{k\to\infty} \omega(k) = \infty, \tag{24}$$

$$\lim_{k\to\infty} \mu(k) = -\frac{1-\delta}{2\delta}. \tag{25}$$

3.2. Phase and group velocities

The phase velocity, which is defined as $v_{ph}(k) = \omega/k$ can be obtained from (21). The group velocity can be calculated by taking the derivative $v_{gr}(k) = d\omega/dk$. The limits of these velocities for large values of k are

$$\lim_{k\to\infty} v_{ph}(k) = \lim_{k\to\infty} v_{gr}(k) = \frac{1}{\sqrt{\delta}} = v_\alpha. \tag{26}$$

Taking into account (8) and (9), one can find the relation between the dimensionless and dimensional values of these velocities. The dimensionless value of $v_{ph} = 1$ corresponds to the dimensional value $V_{ph} = c_s$, and $v_{gr} = v_\alpha$ corresponds to $V_{gr} = c_d$.

In Figs. 3, 4, and 5 the phase and group velocities are plotted against the wave number k. In Figs. 3 and 5 the regions of normal and anomalous dispersion can be distinguished. The regions of normal and anomalous dispersion are separated at the point $k = k_*$. If $k < k_*$ it holds that $v_{ph} > v_{gr}$ (normal dispersion), and if $k > k_*$ it holds that $v_{ph} < v_{gr}$ (anomalous dispersion). The value of k_* is a function of the parameter δ. The numerical analysis shows that the range of values for k_* is $0 \leqslant k_* < \sqrt{3}$. The maximum value of $k_* = \sqrt{3}$ is achieved for $\delta \to 1/9$.

For the value of $\delta \geqslant 0.2$ it was found that $k_* = 0$, and therefore the region of normal dispersion is completely absent and overtaken by the region of anomalous dispersion. Comparison of Figs. 3 and 4 shows the behaviour difference between the group and phase velocities for $\delta < 0.2$ and for $\delta > 0.2$.

3.3. Negative group velocity

The numerical analysis shows that the negative group velocity, shown in Fig. 5, appears only in the region of normal dispersion if $0 < \delta < 0.1345$. The phenomenon of negative group velocity in the microstructured solids was also considered in [5], where the range of the physical parameters, which lead to the appearance of the negative group velocity was derived.

It can be shown that as $\delta \to 0.1345$ the minimum of the group velocity tends to zero. The existence of the negative group velocity in the case of small values of δ is related to the stress–strain relaxation model in the form (3). In this case the hereditary amplitude $\gamma = 1-\delta$ is close to its maximum, and therefore the hereditary features of the wool felt material are expressed most fully.

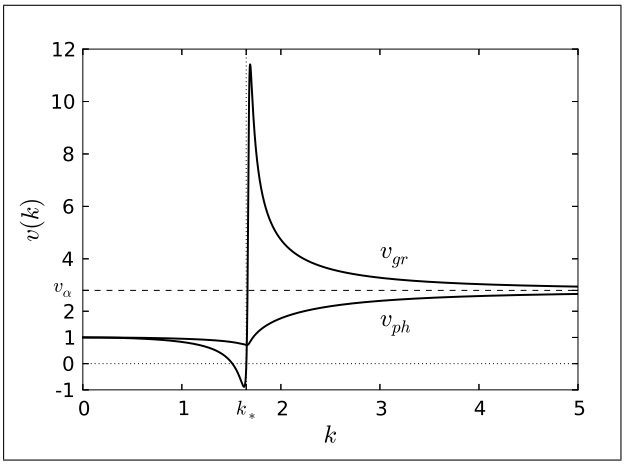

Figure 5. Phase and group velocities calculated for $\delta = 0.128$. Vertical dotted line at k_* separates the regions of normal and anomalous dispersion. Negative group velocity region is located to the left from k_*

The effects of the negative group velocity and anomalous dispersion are always *masked* by the relatively large influence of exponential decay determined by the decay function $\mu(k)$. For example, the spectral wave components k that are associated with strong anomalous dispersion regime ($\delta < 0.2$ and $k > k_*$) are also associated with the large values of the exponential decay $\mu(k)$ (*vide* Fig. 2). This means that in this particular example, anomalous dispersion may be expressed only at the beginning of the wave evolution and only for a short period of time. Most probably, the anomalous dispersion will be overtaken by the normal dispersion regime, with which much smaller decay is associated.

4. Wave attenuation

The aim of this section is to study the rate of a strain pulse attenuation as it propagates along the x-axis. This calls for solution of the boundary value problem (BVP).

4.1. Boundary value problem

The solution to BVP is obtained numerically, by using the finite difference method (FDM). Instead of Eq. (11) we consider a more suitable form of the equation for the finite difference approximation. This form can be obtained by integrating the Eq. (11) over time. This yields

$$\epsilon_{tt} = (\epsilon^p)_{xx} - \gamma \int_0^t (\epsilon^p)_{xx}\, e^{\xi - t} d\xi, \tag{27}$$

where $\gamma = 1-\delta$. The solution of the BVP is solved over the non-negative space domain ($x \geqslant 0$). A boundary value of the strain prescribed at $x = 0$ is selected in the following form:

$$\epsilon(0,t) = A \left(\frac{t}{t_m}\right)^3 e^{3(1-t/t_m)}, \tag{28}$$

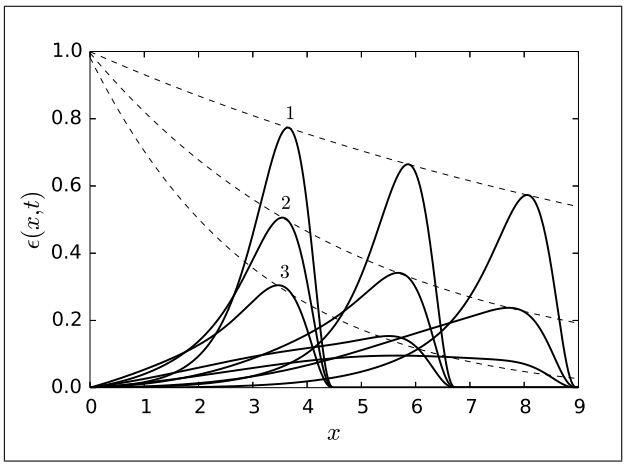

Figure 6. Snapshots of pulses' profiles shown for time moments $t_1 = 4.5$, $t_2 = 6.75$, and $t_3 = 9.0$, varying the parameter δ. The boundary value parameter $t_m = 1/2$. The dashed lines show the amplitude decay. For the pulse 1 ($\delta = 0.8$), the corresponding amplitude decay function is $e^{-0.08x}$; for the pulse 2 ($\delta = 0.5$), the amplitude decay function is $e^{-0.20x}$; for the pulse 3 ($\delta = 0.2$), the amplitude decay function is $e^{-0.32x}$.

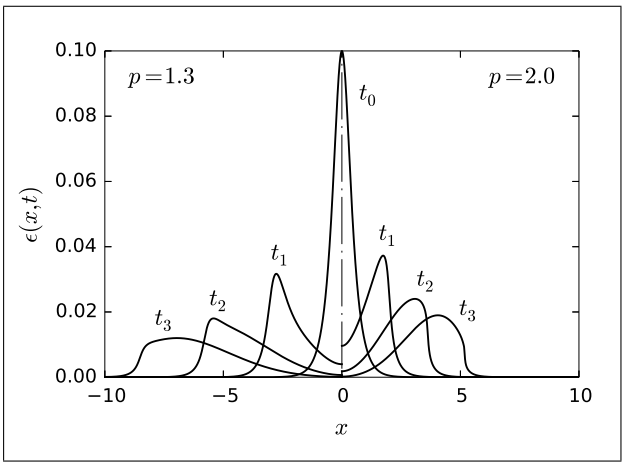

Figure 7. Snapshot of a pulse profiles, where $\delta = 0.5$, $\alpha = 3$, and $A = 0.1$, shown for time moments $t_0 = 0$, $t_1 = 10/3$, $t_2 = 20/3$, $t_3 = 30/3$, calculated for two different values of parameter p.

where t_m defines the time coordinate corresponding to the maximum of a pulse amplitude (peak of the pulse). This form of a pulse is continuous and smooth. At a pulse front the necessary conditions $\epsilon(0,0) = \epsilon_t(0,0) = \epsilon_{tt}(0,0) = 0$ are prescribed. Initially, at $t \leqslant 0$ the felt material is assumed to be at rest, thus $\epsilon(x,0) = \epsilon_t(x,0) = 0$.

Below, the solution to the boundary value problem (27), (28) is presented and analysed.

4.2. Pulse attenuation rate

Figure 6 shows numerical solution of BVP (27), (28), for the linear case, where $p = 1$. The evolution of the form of a pulse determined by the boundary value (28), where the boundary value parameter $t_m = 1/2$, is presented for three sequential time moments, and for three different values of material parameter δ. The dashed lines show corresponding decays of the pulses' amplitudes. These decay curves are plotted through the pulses maxima and fitted to by the exponential function in the form $e^{-\lambda_n x}$, where λ_n is the numerically found exponential decay constant. Here it is suppose that the dominant *fundamental* spectral component ω of a pulse (28) may be estimated from a rough approximation $\omega t_m \simeq 1$.

In [1] it was shown that the values of the decay constants λ_n calculated numerically, and the decay constant $\lambda(\omega)$ taken from the dispersion relation are approximately equal. This means that in principle, this numerical approach can be used to verify the decay constants for any specific value of t_m rather accurately.

5. Nonlinear analysis

In this section, the effects of the nonlinearity of the wool felt material on the wave propagation are considered. We examine the influence of the nonlinearity parameter p, and the effect of an initial pulse amplitude on the evolution of a symmetrical pulse. The analysis is performed in connection with the initial value problem (IVP).

5.1. Initial value problem

The solution of the IVP is solved over the nonnegative time domain ($t \geqslant 0$) of the unbound halfspace. The initial value of the strain prescribed at $t = 0$ is selected in the following form:

$$\epsilon(x,0) = A\,\mathrm{sech}(\alpha x) = \frac{2A}{e^{\alpha x} + e^{-\alpha x}}, \tag{29}$$

$$\epsilon_t(x,0) = \epsilon_x(x,0) = 0, \tag{30}$$

where A is the amplitude, and α is the space parameter.

Below, the numerical solution of the IVP in the form (27), (29), (30) is presented and analysed.

5.2. Influence of the parameter p

Figure 7 shows two solutions of the IVP (27), (29), (30), where only the nonlinearity parameter p is varied, while other parameters are left constant. The solution of the problem is presented for four sequential time moments and for two values of the material parameter p.

The solution of the problem is symmetric with respect to $x = 0$, because the initial value (29) is an even bell-shaped function. The half of the solution, where $p = 1.3$ is plotted to the left side from the axis of symmetry marked by the dot-dashed line in Fig. 7,

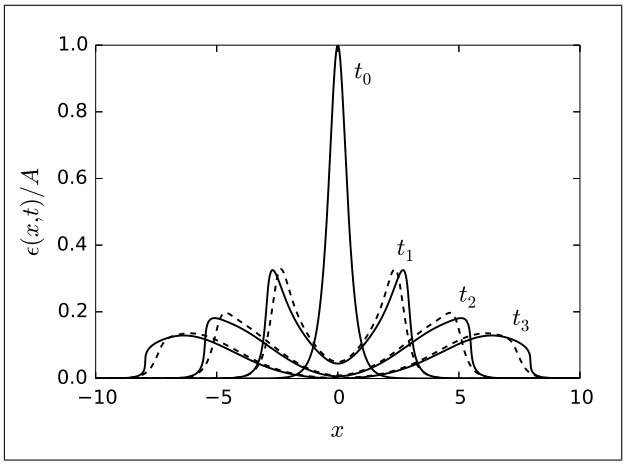

Figure 8. Normalized snapshots of pulse profiles, where $\alpha = 3$, $\delta = 0.5$ and $p = 1.45$, shown for time moments $t_0 = 0$, $t_1 = 10/3$, $t_2 = 20/3$, $t_3 = 30/3$. The profile starting with initial amplitude $A = 0.2$ is shown by solid line. The profile starting with initial amplitude $A = 0.02$ is shown by dashed line.

and the half of the solution, where $p = 2.0$ is plotted to the right side.

Figure 7 shows that the front part of a pulse becomes steeper as it propagates through the felt material. The process of the pulse steepening is greater for the felt with larger value of the parameter p. Accumulation of this effect results in the eventual pulse breaking. This means that a shock wave will be formed, and the shock wave formation is brought to an earlier time for the larger values of p. In addition, a strong attenuation of the pulse amplitude with progression of time is visible.

5.3. Influence of the initial amplitude

Figure 8 shows that a forward-facing slope of a pulse is strongly dependent on the pulse amplitude A. For larger amplitude, the maximum point or the peak of a pulse propagates faster than its front. This phenomenon prevails with the increasing of the amplitude of the initial value disturbance. The accumulation of this effect results in the eventual shock wave formation. The progressive forward leaning of a propagating pulse can be explained by the fact that the group velocity is greater than the phase velocity. Also, these phenomena are related to the nonlinear features of the felt material.

6. CONCLUSIONS

The nonlinear felt model that takes into account the elastic and hereditary properties of the microstructured felt was used to study a strain pulse evolution in the one-dimensional case. The linear and nonlinear analysis of the model was presented.

The numerical solution of the linear boundary value problem was used to estimate a strain pulse amplitude decay during its propagation through the felt. It was concluded that in the linear case the exponential decay constants may be obtained rather accurately by using dispersion analysis.

The result of dispersion analysis of the linear problem showed that normal and anomalous dispersion types can exist in the wool felt material. It was confirmed that for some values of the parameters the negative group velocity region appears. The negative group velocity emerged always in connection with the region of normal dispersion.

The nonlinear effects of the general influence of the nonlinearity parameter p, and the amplitude of an initial disturbance were demonstrated. It was shown that for the higher value of the nonlinearity parameter p the front of an evolving pulse become steeper, and this phenomenon was intensified with the growth of the value of the parameter p. Also, it was shown that the front slope of an evolving pulse was strongly determined by the pulse amplitude. A greater initial amplitude forced the peak of the pulse to propagate faster than its front. Therefore, these nonlinear effects were eventually responsible for the appearance of the discontinuity at a pulse front and the formation of a shock wave.

This paper presents a novel wave equation that describes many physical effects that can be observed in the microstructured wool felt. The most dominating feature of the felt was demonstrated to be the strong damping effect on any wave evolving and propagating through it.

Acknowledgement

This research was supported by the EU through the European Regional Development Fund, and by the Estonian Ministry of Education and Research (SF 0140077s08). Conference travel expenses of the first author where financed by Kristjan Jaak scholarship (Archimedes Foundation, Estonia). The authors would like to thank Prof. Aleksander Klauson from Tallinn University of Technology for his assistance in the stress–strain testing of the felt pads.

References

[1] D. Kartofelev, A. Stulov: Propagation of deformation waves in wool felt. ACTA Mechanica, Online first, (2014) [1–11].

[2] A. Stulov: Hysteretic model of the grand piano hammer felt. J. Acoust. Soc. Am. **97** (4) (1995) 2577–2585.

[3] N. Yu. Rabotnov: Elements of hereditary solid mechanics. Chap. 17. Moscow: MIR Publishers, 1980.

[4] A. Stulov: Experimental and computational studies of piano hammers. Acta Acustica united with Acustica **91** (6) (2005) 1086–1097.

[5] T. Peets, D. Kartofelev, K. Tamm, J. Engelbrecht: Waves in microstructured solids and negative group velocity. EPL - A Letters Journal Exploring the Frontiers of Physics, **103** (1) (2013) 16001-p1–16001-p6.